

# Interaction of Multiple Supersonic Jets with a Transonic Flowfield

Jonah Manela\*

*Armaments Development Authority, Haifa, Israel*

and

Arnan Seginer†

*Technion—Israel Institute of Technology, Haifa, Israel*

The influence of multiple high-pressure, supersonic, radial or tangential jets injected from the circumference of the base plane of an axisymmetric body on its longitudinal aerodynamic coefficients in transonic flow is studied experimentally. The interaction of the jets with the body flowfield increases the pressure on the forebody, thus altering its lift and static stability characteristics. It is shown that, within the range of parameters studied ( $0.7 \leq M_\infty \leq 1.05$ ;  $20 \leq P_{0j}/P_\infty \leq 70$ ;  $0 \leq \alpha \leq 18^\circ$ ), this interaction has a stabilizing effect on the body. The contribution to lift and stability is significant at small angles of attack and decreases nonlinearly at higher angles when the cross-flow mechanism becomes dominant.

## Nomenclature

$C_N$	= normal force coefficient, $N/qS$
$C_p$	= pressure coefficient, $(p - p_\infty)/q$
$d^*$	= nozzle diameter
$D$	= body diameter, also drag
$h$	= jet penetration height
$M$	= Mach number
$N$	= normal force
$p$	= pressure
$q$	= freestream dynamic pressure
$S$	= body cross-sectional area, $\pi D^2/4$
$X$	= streamwise distance measured upstream from jets
$\alpha$	= angle of attack
$\phi$	= circumferential angle

## Subscripts

CP	= center of pressure
$j$	= jet parameters
$t$	= nozzle throat parameters
0	= stagnation conditions
$\infty$	= freestream conditions

## Introduction

THE interaction of transverse jets with the ambient flowfield (e.g., in STOL aircraft, thrust vector control, and direct vehicle attitude control) is characterized by an effective jet thrust that is larger than the conventional thrust based on the jet momentum alone. Most experimental studies of this phenomenon concentrated on the interaction of a single, usually sonic, two-dimensional jet with an external supersonic flow.

The typical features of such an interaction flowfield are described by Spaid and Zukosky.<sup>1</sup> The jet acts as an obstacle to the main flow, generating a shock wave and forcing the flow to separate and lift off the surface in order to negotiate

the obstacle. The separation shock generates a sharp pressure rise, followed by a pressure plateau. A bow shock that forms near the jet causes an additional pressure rise after the plateau. The jet is bent aft by the high-pressure region and a low-pressure separation region forms behind it. Farther downstream, the combined jet and outer flows reattach through a recompression shock.

The three-dimensional interaction of a circular jet with a supersonic planar flow is, generally speaking, similar to the two-dimensional interaction described above. However, the extent and intensity of the three-dimensional interaction is reduced because the flow can go around the obstacle in addition to going over it. The interactions of a single circular jet and of multiple circular jets with a planar flow were studied by Spaid et al.<sup>2</sup> and their results are summarized in Ref. 3.

While most of the research effort concentrated on supersonic interactions that were common in thrust vectoring and direct attitude control of missiles, very little work was done on transonic interactions. The scant available information<sup>4</sup> shows that the transonic interaction is, generally speaking, similar in character to the previously described supersonic one. The main differences are that the pressure gradients are weaker, the pressure plateau is very short and vanishes at low injection pressure ratios, and the shock waves are weak normal shocks.

With the development of STOL fighter aircraft and guided and maneuvering munitions, the interest in transonic interactions increased. Therefore, the present investigation was concerned with an interaction that has not been studied previously, namely that of several circular supersonic jets with an external transonic flow. A further difference from previous studies is that they dealt with injection from a flat plate into a planar flow, whereas in this study a number of circular, radial jets are injected symmetrically from the perimeter of the base of an axisymmetrical body into a three-dimensional outer flow. Thus, in the present case, the jets do not generate any direct net forces or moments on the body. The forces and moments that were actually measured when the body was positioned in the flow at an angle of attack were a result of small pressure differences between the interaction regions on the windward and leeward sides of the body.

The main purpose of this investigation was to gather information on the effects of the jet interaction with transonic flow on the aerodynamic characteristics of the body and their dependence on the various flow and jet parameters. Results presented here show that the interaction generates additional lift and increases the longitudinal static stability of the body at low angles of attack.

Presented as Paper 83-1680 at the AIAA 16th Fluid and Plasma Dynamics Conference, Danvers, MA, July 12-14, 1983; received Nov. 1, 1984; revision received April 8, 1985. Copyright © American Institute of Aeronautics and Astronautics, Inc., 1985. All rights reserved.

\*Research Scientist.

†Associate Professor, Department of Aeronautical Engineering (National Research Council Senior Research Associate at NASA Ames Research Center, Cleveland, at the time of paper presentation and submission). Member AIAA.

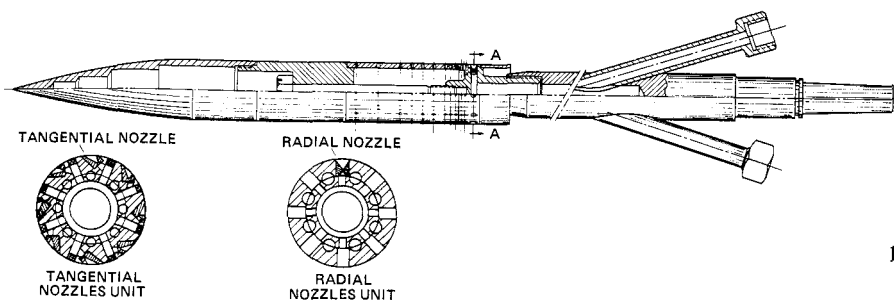


Fig. 1 Details of the wind tunnel model.

Most of the experiments were conducted with radial jets, but several tests were made with jets that were injected tangentially to the base circumference. Such jets could be used to generate high spin rates. No fundamental difference was observed between the results of the radial injection and the tangential injection, except for the rolling moments produced by the latter.

### Experimental Setup, Tests, and Data Reduction

#### Apparatus

The experiments were conducted on an 8-caliber, 45-mm-diam. ogive cylinder model with a 3-caliber ogive nose section and a 5-caliber cylindrical body (Fig. 1). The base section of the model included the injection nozzle units. Two interchangeable nozzle units were employed, one having eight radial nozzles and the other having eight tangential nozzles (Fig. 1). All the nozzles were convergent-divergent supersonic nozzles. Seven out of the eight nozzles could be plugged for single-nozzle preliminary experiments. Seventy-seven pressure taps were drilled into the model, upstream of the nozzles along several generatrices. Most of the pressure taps were located on one side only of the model's pitch plane. Four pressure taps were located on the other side to validate the symmetry of the flow with respect to the angle-of-attack plane. The general arrangement of the pressure taps is shown in Fig. 1. A more detailed description of the test apparatus is given in Refs. 5 and 6.

#### Tests

##### Single-Jet Tests

A series of preliminary wind tunnel tests was conducted to validate the experimental apparatus and the data reduction software. In these tests, a single jet was injected from the nozzle on the upper generatrix ( $\phi = 0$  deg). Seven pressure taps along this generatrix were continuously monitored by individual pressure transducers. The tests were conducted at constant angles of attack of  $\alpha = 0, 9$ , and  $-9$  deg, with the Mach number varying continuously from 0.4 to 1.1. The nominal injection pressure was  $p_{0j} = 40$  atm. The injection pressure ratio ( $p_{0j}/p_\infty$ ) varied between 44 and 89, owing to the change in freestream static pressure with increasing Mach number.

##### Multiple-Jet Tests

These tests were performed with various combinations of the nominal values of the test parameters:

- 1) Angle of attack  $\alpha = -5, 0, 5, 10, 15, 18$  deg.
- 2) Injection pressure ratios  $p_{0j}/p_\infty = 20, 40, 60-70$ .
- 3) Mach numbers  $M_\infty = 0.8, 0.9, 1.0$ .

#### Data Reduction: Aerodynamic Coefficients

In addition to the test parameters (including the jet mass flux), only pressure data on the model were recorded. Pressures were reduced to the conventional local pressure coefficients

$$C_p = (p - p_\infty) / [\frac{1}{2}(\gamma_\infty p_\infty M_\infty^2)] \quad (1)$$

The pressure distributions in the circumferential and axial directions were smoothed and integrated to give the normal force coefficient  $C_N$  and the upstream distance of the center of pressure  $X_{CP}/D$  from the injection plane,

$$C_N = -\frac{4}{\pi} \int_0^2 \int_0^\pi \left[ C_p \left( \phi, \frac{X}{D} \right) \cos \phi d\phi \right] d\frac{X}{D} \quad (2)$$

$$\frac{X_{CP}}{D} = -\left( \frac{4}{\pi C_N} \right) \int_0^2 \int_0^\pi \left[ C_p \left( \phi, \frac{X}{D} \right) \cos \phi d\phi \right] \frac{X}{D} d\frac{X}{D} \quad (3)$$

The integration was performed over the 2-diam long metric section only.

### Results and Discussion

#### Single-Jet Tests

The pressure distributions upstream of the jet (Fig. 2) are typical of transonic flow.<sup>4</sup> The pressure increases gradually as the jet is approached. No pressure plateau is observed. Both the pressure levels and the upstream extent of the interaction are increasing with increasing freestream Mach number and injection pressure ratio. These two parameters could not be varied independently in the blowdown tunnel because of the continuous variation of the Mach number in the single-jet tests. Note that the pressures are higher at both the positive and negative angles of attack ( $\alpha = \pm 9$  deg) than at  $\alpha = 0$  deg. This is an indication of the highly nonlinear character of the interaction (discussed below). The slightly higher pressures at the negative angle of attack ( $\alpha = -9$  deg) than at the positive ( $\alpha = 9$  deg) predict the increased static stability that is later observed in the multiple-jet tests.

The single-jet data were compared, as a validation of the apparatus and data-reduction system, with the data of Ref. 3 (Fig. 3). These data were normalized by an empirical penetration height  $h_c/d_i = 0.695(p_{0j}/p_\infty)^{1/2}$  that was suggested by Ref. 7 as the distance from the nozzle to the first Mach disk in a supersonic injection into a fluid at rest. The agreement is rather good in spite of the jet in Ref. 3 being injected from the ogive cylinder junction and not at the base, as on the present model.

#### Multiple-Jet Tests

Typical pressure distributions with eight active jets at  $M_\infty = 0.9$  and  $p_{0j}/p_\infty = 65-67$  are presented in Figs. 4 and 5 for  $\alpha = 0$  and  $10.1$  deg, respectively. At  $\alpha = 0$  deg (Fig. 4), the flow is nearly axisymmetric. The only deviations from an axisymmetric flow are measured very close to the injection nozzles where high pressures are observed in line with the nozzle and lower pressures are observed between the nozzles. These local variations are in agreement with the single- and dual-circular-jet results of Refs. 2 and 3. The pressure gradually increases as the nozzles are approached, except at the pressure taps between the nozzles in the last 0.2 body diameters. At  $\alpha = 10.1$  deg, the effect of the crossflow can be seen, in addition to that of a stronger interaction between the jets and the outer flow (Fig. 5). One can observe (as in Fig. 2) that the pressures on the windward side ( $\phi = 180$  deg) are slightly higher than those

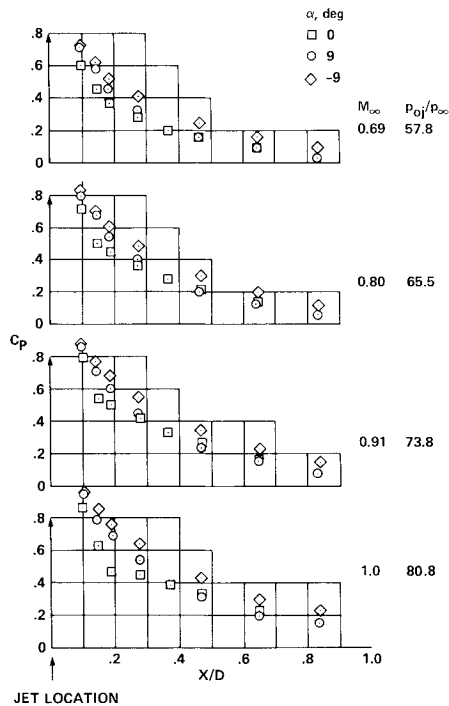


Fig. 2 Single-jet pressure distributions.

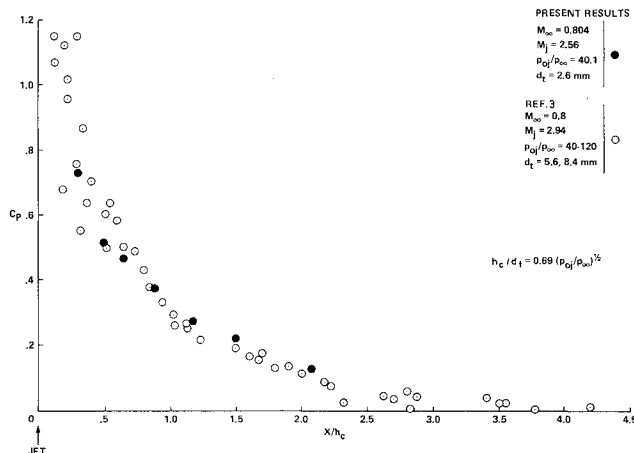


Fig. 3 Single-jet results compared with data from Ref. 3.

on the leeward side ( $\phi = 0$  deg). The results shown in Figs. 4 and 5 are characteristic and are shown as an example. Additional pressure distributions, obtained for different test conditions, are presented in Ref. 6.

The variation of the normal force coefficient with the angle of attack is shown in Fig. 6 for various Mach numbers and injection pressure ratios. Also shown in Fig. 6 are the conventional normal force results without injection. These compare very well with the predictions of the cross-flow theory,<sup>8</sup> except for the experimentally observed increase with increasing Mach number. The normal force induced by the interaction of the jets with the outer flow is larger than that induced by the cross-flow alone (Fig. 6), especially at the lower angles of attack ( $0 < \alpha < 5$  deg). These jet-induced normal force increments diminish at the higher angles of attack. The apparent scatter in the data in Fig. 6 could be due to the simultaneous variation of the Mach number and injection pressure ratio. The data are therefore replotted in Fig. 7 as a function of the injection pressure ratio for various Mach numbers and angles of attack. When one takes into account the angle-of-attack effect (of Fig. 6), only a weak influence of the injection pressure

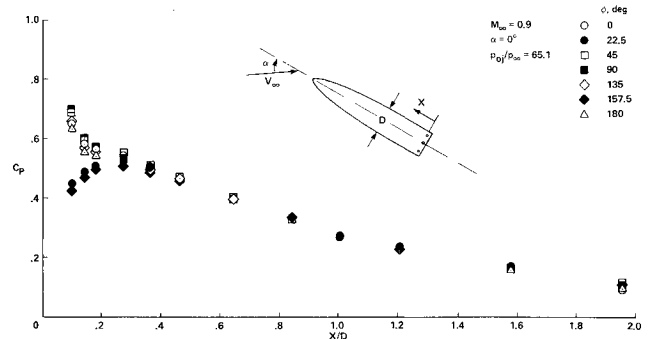
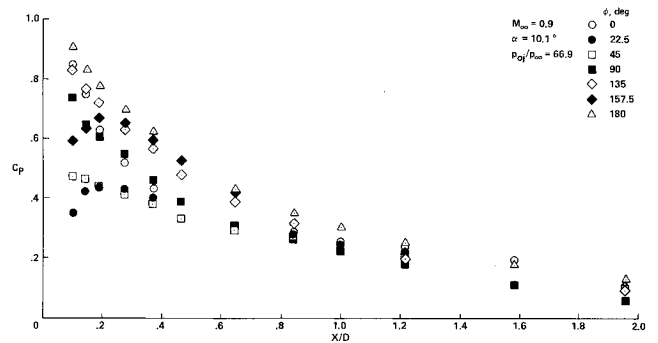
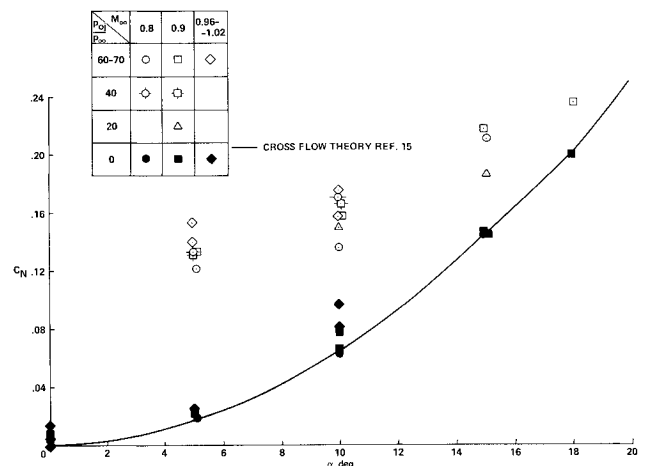
Fig. 4 Pressure distribution at  $\alpha = 0$  deg for eight radial jets.Fig. 5 Pressure distribution at  $\alpha = 10.1$  deg for eight radial jets.

Fig. 6 Normal force coefficient variations with angle of attack.

ratio on the normal force is found (for  $20 \leq P_{0j}/P_{\infty} \leq 70$ ). Most of the apparent scatter in Fig. 6 must, therefore, be a Mach number effect, with the normal force increasing when the Mach number is increased (for  $0.8 \leq M_{\infty} \leq 1.02$ ).

The downstream displacement of the center-of-pressure location (of the metric section of the model only), caused by the jet-induced interaction, is shown in Fig. 8 as a function of the angle of attack for various Mach numbers and injection pressure ratios. This displacement is largest around  $\alpha = 5$  deg and decreases rapidly as the angle of attack is increased. The effect of the interaction, like its influence on the normal force (Fig. 6), seems to vanish for  $\alpha > 20$  deg where the cross-flow apparently dominates the flowfield and the jet-induced interaction becomes insignificant. When the center-of-pressure data are replotted as a function of the injection pressure ratio (Fig. 9), it is found that the downstream displacement of the center of pressure increases when the injection pressure is

increased. The Mach number effect on this phenomenon seems to be small.

Although the dependence of the normal force [the integral of the pressure distribution, Eq. (2)] on the injection pressure ratio is quite weak (Fig. 7), its effects on the pressure distribution itself are significant (Fig. 10). This interesting result indicates that the pressure distribution merely shifts while it maintains a constant average. This shifting is reflected in the aft movement of the center of pressure with increasing injection pressure ratio (Fig. 9).

The pressure distributions obtained with a single jet and with eight jets are compared in Fig. 11 at approximately identical test conditions. The pressure field induced by the eight jets is much stronger and has a much more extensive influence (more than double) than the single-jet field and, in that, resembles the flowfield induced by a two-dimensional jet.<sup>1-3</sup>

A better understanding of the behavior of the normal force (Fig. 6) can be obtained from a crossplot of the streamwise pressure distributions at various angles of attack. Figure 12 shows the variation of the pressures with the angle of attack at fixed axial stations along the upper generatrix ahead of the jet for constant nominal test conditions. Also shown for comparison is the pressure variation with the angle of attack without blowing, which does not change with  $X/D$  on this section of the model. The interaction field can be roughly divided into two regions of different character. The first is the far upstream region ( $X/D \gtrsim 0.5$ ). There, the pressure variation generally resembles the cross-flow-induced variation without injection. The pressure levels are, of course, higher than without injection, and increasing in the downstream direction

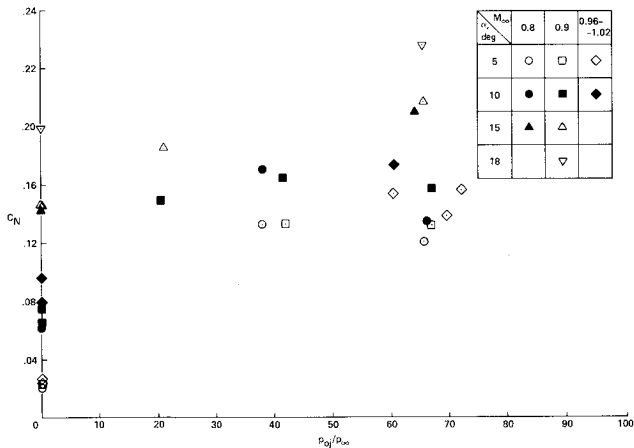


Fig. 7 Pressure ratio effects on the normal force coefficient.

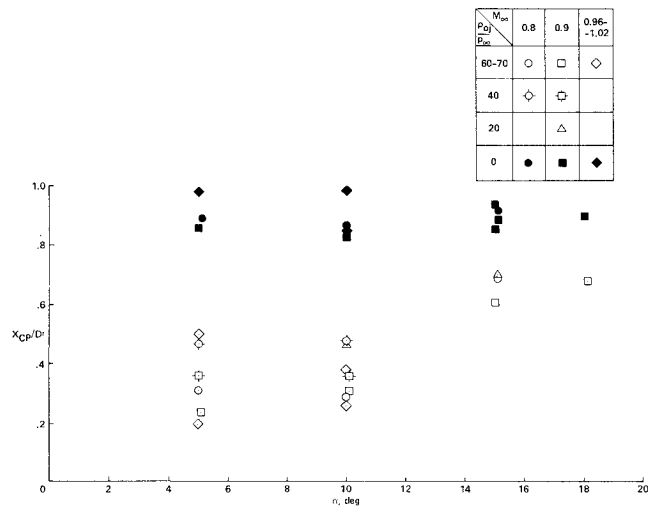


Fig. 8 Center-of-pressure location variation with angle of attack.

because of the free-flow retardation by the jets' obstacle. In the near region ( $X/D \lesssim 0.5$ ) the jet disturbance is the dominant factor and the pressure variation differs significantly from the cross-flow type. The pressure variation with the angle of attack is highly nonlinear and has a sharp minimum in the vicinity of  $\alpha \approx 5$  deg. This minimum is the reason for the very rapid increase in the contribution of the interaction pressure field to the normal force when the angle of attack is increased from 0 to 5 deg (Fig. 6) and for its diminishing at higher angles of attack. It also explains why the pressures in Fig. 2 for both  $\alpha = 9$  and  $-9$  deg were higher than those at  $\alpha = 0$  deg.

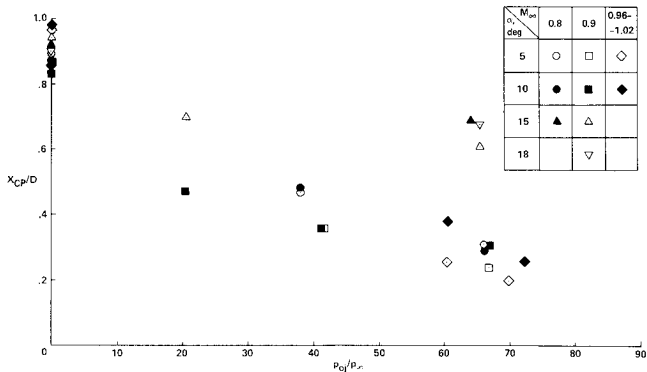


Fig. 9 Pressure ratio effects on the center-of-pressure location.

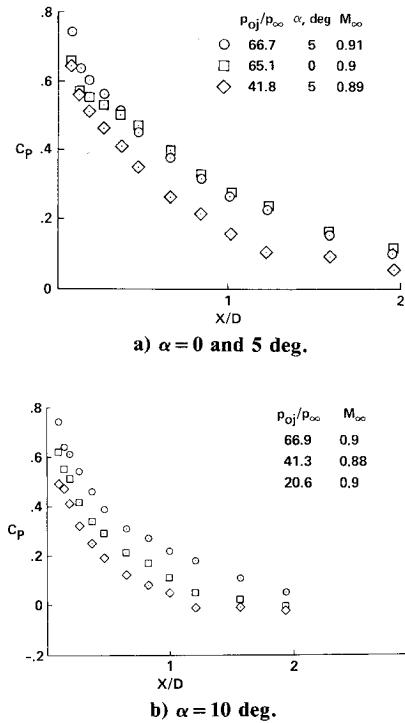


Fig. 10 Pressure ratio effects on the pressure distributions.

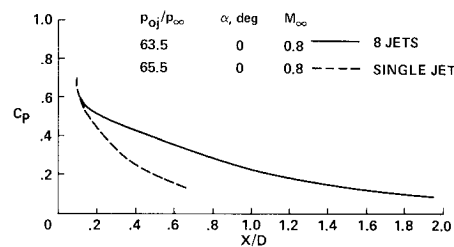


Fig. 11 Pressure distributions of a single jet and of eight jets.

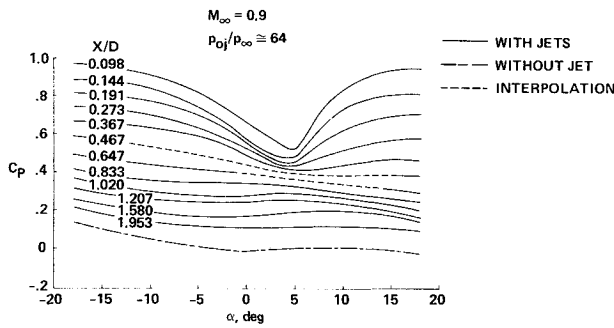


Fig. 12 Pressure variation with angle of attack in fixed locations.

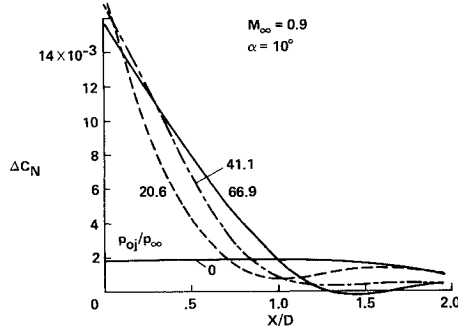


Fig. 13 Normal force coefficient distribution variation with injection pressure ratio.

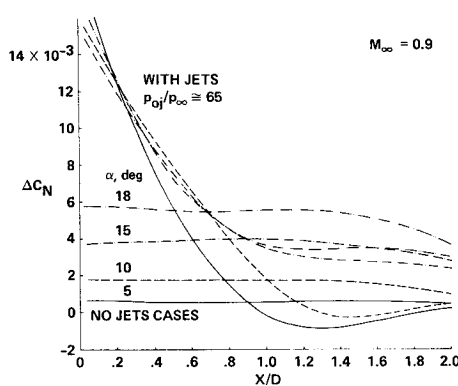
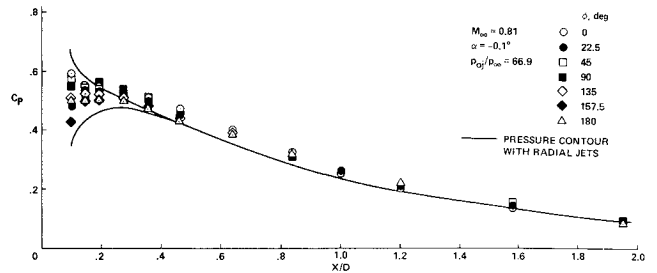
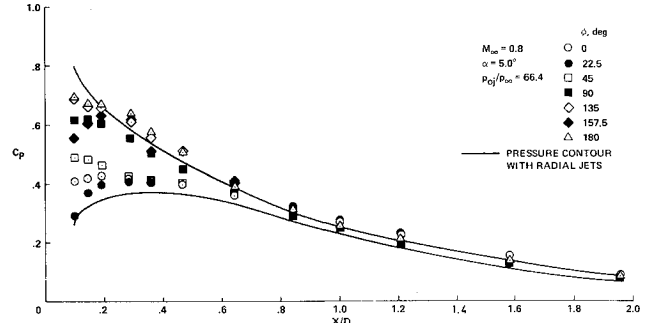


Fig. 14 Normal force coefficient distribution variation with angle of attack.

Another interesting result (Fig. 13) is the normal force distribution along the body at  $M_\infty = 0.9$  and  $\alpha = 10^\circ$  for several injection pressure ratios (including  $p_{oj}/p_\infty = 0$ ). The increasing pressure ratio increases the pressure loading on a body section near the jets of about 1 diam length but reduces the load farther upstream, with even some locally negative lift at the highest injection pressure. The overall result of this change in the distribution is that the total normal force (the integral under the curves in Fig. 13) changes very little with varying pressure ratio (for  $20 \leq p_{oj}/p_\infty \leq 70$ , as in Fig. 7) compared with the pressure distribution itself (Fig. 10), so that the center of pressure moves aft, closer to the jets, as was also observed in Fig. 9. When similar normal force distribution curves, all with the same injection pressure ratio, are plotted for several angles of attack (Fig. 14), the influence of the angle of attack is not monotonous, as was that of the injection pressure. The interaction contributes significantly to the normal force at low angles of attack ( $\alpha < 10^\circ$ ), with the maximum contribution in the vicinity of  $\alpha \approx 5^\circ$ . At higher angles of attack, this contribution diminishes very rapidly and the normal force is increasingly governed by the cross-flow mechanism. At  $\alpha = 18^\circ$



a) Pressure distribution at  $\alpha \approx 0^\circ$ .



b) Pressure distribution at  $\alpha = 5^\circ$ .

Fig. 15 Comparison of tangential injection with radial injection.

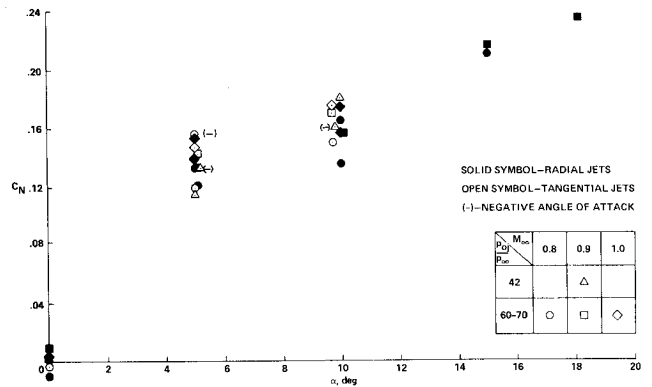


Fig. 16 Tangential injection: normal force coefficient variation with angle of attack.

deg (the maximum angle of attack considered in these tests), the jet interaction contributed only 15% of the total normal force acting on the cylindrical segment upstream of the jets, whereas at  $\alpha = 5^\circ$  the interaction contributed about 85% of the total normal force. Similar results can also be seen in Fig. 6.

### Tangential Injection

The tests with the tangential jets were considered necessary because it seemed that for identical test conditions the disturbance to the outer flow presented by tangential jets should be smaller than that of radial jets. This expectation turned out to be incorrect. Typical pressure distributions at  $\alpha \approx 0$  and  $5^\circ$  are compared with the corresponding pressure distributions obtained with radial jets (Figs. 15a and 15b, respectively) and are found to be very much alike, except for small differences in the region near the jets. One must conclude, therefore, that because the circumferential disturbance of the jets is nearly two-dimensional (Fig. 11), the direction of injection makes hardly any difference as long as the mass flux and injection pressure ratio are the same in both cases. It is not surprising, therefore, that the normal force and center-of-pressure dependence on Mach number, injection pressure ratio, and

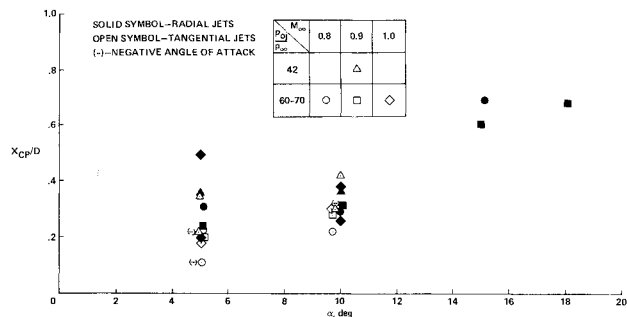


Fig. 17 Tangential injection: center-of-pressure location variation with angle of attack.

angle of attack is also similar to that of the radial jet case (Figs. 16 and 17). The differences between the results of the two modes of injection are within the scatter of the experimental data.

### Conclusions

The interaction of a transonic free flow with eight circular jets, injected into the flow around the perimeter of the base of an axisymmetric body, was studied experimentally. Radial and tangential injection modes were investigated.

The pressure field induced on the section of the body upstream of the jets contributes a net positive normal force and moves the longitudinal center of pressure aft when the blowing is turned on at  $p_{0j}/p_\infty = 20$ . The normal force is relatively insensitive to changes in the injection pressure ratio (within the range  $20 \leq p_{0j}/p_\infty \leq 70$ ). However, the pressure distribution does change, so that the center of pressure moves farther aft toward the jets with increasing pressure ratio.

The dependence of the pressure field and the normal force on the angle of attack is highly nonlinear. This is apparently a result of flow separation from the leeward side of the body at angles of attack larger than 5 deg. The largest contribution of the interaction to the normal force occurs in the vicinity of  $\alpha \approx 5$  deg and diminishes rapidly when the angle of attack is increased. The cross-flow mechanism dominates the flowfield for higher angles of attack, apparently resulting from the existence of separated flow above the upper surface of the body.

No significant differences between the results of radial injection and tangential injection were found.

### References

- <sup>1</sup>Spaid, F.W. and Zukoski, E.E., "A Study of the Interaction of Gaseous Jets from Transverse Slots with Supersonic External Flows," *AIAA Journal*, Vol. 6, Feb. 1968, pp. 205-212.
- <sup>2</sup>Spaid, F.W., Zukoski, E.E., and Rosen, R., "A Study of Secondary Injection of Gases into a Supersonic Flow," NASA TR-32-834, 1966.
- <sup>3</sup>Spaid, F.W. and Cassel, L.A., "Aerodynamic Interference Induced by Reaction Controls," AGARD AG-173 (AD-775209), 1973.
- <sup>4</sup>Heyser, A. and Maurer, F., "Experimentelle Untersuchungen an festen Spoilern und Strahlspoilern bei Machschen Zahlen von 0.6 bis 2.8," *Zeitschrift fuer Flugwissenschaften*, Vol. 10, Heft 4/5, 1962.
- <sup>5</sup>Seginer, A. and Manela, J., "Interaction of Multiple Supersonic Jets with a Transonic Flow Field," NASA TM 84369, May 1983 (also AIAA Paper 83-1680, July 1983).
- <sup>6</sup>Manela, J., "The Influence of Jets, Injected Transversely into a Transonic Flow Near the Base of an Axisymmetric Configuration, on Flow Field, Lift and Stability Characteristics of the Body," M.Sc. Thesis, Technion—Israel Institute of Technology, Haifa, Nov. 1980.
- <sup>7</sup>Crist, S., Sherman, P.M., and Glass, D.R., "Study of the Highly Under-Expanded Sonic Jet," *AIAA Journal*, Vol. 4, Jan. 1966, pp. 68-71.
- <sup>8</sup>Jorgensen, L.H., "Prediction of Static Aerodynamic Characteristics for Slender Bodies Alone and With Lifting Surfaces at Very High Angles of Attack," NASA TMX-M3123, July 1976.